

Reduction of switching current density in perpendicular magnetic tunnel junctions by tuning the anisotropy of the CoFeB free layer

M. T. Rahman,^{1,a)} A. Lyle,¹ P. Khalili Amiri,² J. Harms,¹ B. Glass,¹ H. Zhao,¹ G. Rowlands,³ J. A. Katine,⁴ J. Langer,⁵ I. N. Krivorotov,³ K. L. Wang,² and J. P. Wang¹

¹Department of Electrical and Computer Engineering, MINT Center, University of Minnesota, Minneapolis, Minnesota 55455, USA

²Department of Electrical Engineering, University of California at Los Angeles, Los Angeles, California 90095, USA

³Department of Physics and Astronomy, University of California at Irvine, Irvine, California 92697, USA

⁴Hitachi Global Storage Technologies, San Jose, California 95135, USA

⁵Singulus Technologies, Kahl am Main 63796, Germany

(Presented 31 October 2011; received 23 September 2011; accepted 1 November 2011; published online 28 February 2012)

The spin torque switching behavior of perpendicular magnetic tunnel junctions consisting of a CoFeB free layer and a CoFeB/Ru/(Co/Pd)_n exchanged coupled fixed layer is investigated. At first, the Ru and CoFeB layer thickness is tuned in the CoFeB/Ru/(Co/Pd)_n structure to form a ferromagnetically exchange coupled structure with a strong PMA at an annealing treatment of 325 °C for 1 h. Then it is shown that the CoFeB free layer thickness plays an important role in the switching current density. The switching current density decreases with the increase of the CoFeB free layer thickness. A minimum switching current density of 1.87 MA/cm² is achieved for a device with 60 nm diameter. The mechanism involved in the switching current reduction with the decrease of CoFeB free layer thickness is also studied. © 2012 American Institute of Physics. [doi:10.1063/1.3673834]

I. INTRODUCTION

Spin transfer torque^{1,2} random access memory (STT-RAM) has been studied intensively^{3–9} to address the scalability and higher power consumption issues of magnetic random access memory. In order to further improve the scalability, a spin transfer torque (STT) cell with perpendicular anisotropy has been proposed and demonstrated.^{3,10–12} Co/M (M = Pd, Pt) multilayers (MLs) have been reported as a potential material for perpendicular magnetic tunnel junctions (PMTJs)^{13–17} due to its strong perpendicular anisotropy and high temperature annealing stability.¹⁵ However, these (Co/M) MLs are not suitable as the free layer due to its high damping constant and (111) texture. Recently, PMA has been reported in a Ta/CoFeB-MgO-CoFeB/Ta structure and a PMTJ has been demonstrated using this structure.^{18–20} One of the remaining challenges with this structure is to clearly define a fixed layer that has a coercivity much greater than the free layer. The CoFeB layer needs to be sandwiched by Ta and MgO for the PMA in this structure, therefore it is not possible to use an antiferromagnetic coupling layer to pin the fixed layer. This work reports on a PMTJ structure using (Co/Pd)_n/Ru/CoFeB as the fixed layer instead of a single CoFeB layer.

Another major MTJ development challenge in STT-RAM technology is to reduce the write current density. A large switching current density increases the transistor size required for write operation thus limiting the memory den-

sity, as well as increasing the write voltage, affecting energy dissipation and device endurance. Several groups^{3,22–24} have reported that the switching current density can be significantly lower in STT-RAM with PMTJ structure when compared to the in-plane one. Reduction of switching current has also been demonstrated by combining a perpendicular polarizer with an in-plane MTJ.^{25,26}

This work demonstrates the development of a PMTJ stack using (Co/Pd)_n/Ru/CoFeB as the fixed layer and CoFeB as the free layer. Moreover, we explore an effective route to further reduce the switching current density in this PMTJ structure by tuning the free layer PMA.

II. EXPERIMENTAL PROCEDURES

The materials stacks were deposited in a Singulus TIMARIS physical vapor deposition system. The magnetic properties at the film level were measured with a vibrating sample magnetometer. Circular PMTJ junctions with 60 nm diameter were fabricated by electron beam lithography and an ion milling process. The transport properties were measured by using a standard GSG probe at room temperature. The composition of CoFeB in this work is used as Co₂₀Fe₆₀B₂₀.

III. RESULTS AND DISCUSSION

At first we develop Sub/MgO/CoFeB/Ru/{Co/Pd}_n layers with perpendicular anisotropy by engineering the exchange coupling between CoFeB and (Co/Pd) MLs. Figures 1(a) and 1(b) show out-of-plane *M*-*H* loop of optimized structure with Sub/MgO (0.8 nm)/CoFeB (1.5 nm)/Ru (0.3 nm)/Co [(0.3 nm)/Pd (1 nm)]₃/Ta (5 nm) layer structure in

^{a)}Author to whom correspondence should be addressed. Electronic mail: rahma070@umn.edu.

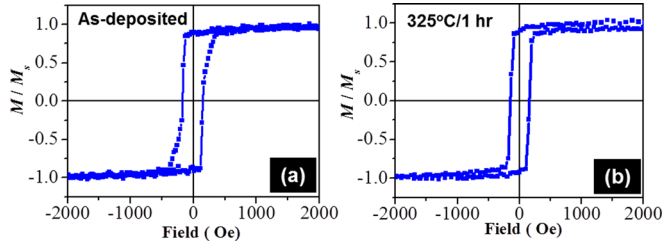


FIG. 1. (Color online) Out-of-plane M - H loop of Sub/MgO (0.8)/CoFeB (1.5 nm)/Ru (0.3 nm)/Co [(0.3 nm)/Pd (1 nm)]₃/Ta (5 nm) film at (a) as-deposited state and (b) after annealing at 325 °C for 1 h.

as-deposited and post-annealed at 325 °C for 1 h. These results can be explained from the viewpoint of energy balance between the (Co/Pd)_n layers and the CoFeB layers. The net anisotropy direction in the (Co/Pd)_n/CoFeB system comes from the competition between the interface anisotropy in (Co/Pd)_n and the demagnetization field in CoFeB. The (Co/Pd)_n/CoFeB system exhibits strong PMA as the interface anisotropy²⁷ of (Co/Pd)_n overcomes the demagnetization field of the CoFeB. These M - H loops also indicate that the CoFeB and (Co/Pd)_n layers are ferromagnetically coupled through 0.3 nm Ru. The thin Ru layer is inserted to block the templating of the (110) texture^{15,28} into CoFeB from (111) textured (Co/Pd) MLs as well as to get a smooth MgO/CoFeB interface and better crystallinity.

Hereafter, we develop the full stack PMTJ structure with Sub/bottom electrode/Ta (5 nm)/CoFeB (1.0–2.0 nm)/MgO (0.8 nm)/CoFeB (1.5 nm)/Ru (0.3 nm)/[Co (0.3 nm) Pd (1 nm)]₁₀/(top electrode) and anneal at 200 °C for 2 h. Then circular MTJ junctions were fabricated with 60 nm diameter and spin torque induced switching is studied. Typical resistance hysteresis loops of field (R versus H) and current driven (R versus H) switching are shown in Figs. 2(a) and 2(b), respectively, for a MTJ junction with CoFeB free layer thickness of around 1.0 nm. The well-defined switching behavior between parallel and anti-parallel magnetization states exhibited in R - H loop indicates good PMA in the CoFeB free layer. However, the R - H loop exhibits an offset field due to the combined effect of orange-peel coupling and dipolar field from the fixed layer that can be eliminated by using SAF fixed layer.^{21,24} The perpendicular magnetoresistance (MR) ratio estimated from the R - H loop is around 20%. The low MR value may be due to the low annealing temperature (200 °C) for this specific sample. A quasistatic tester with pulse voltage capability (HP8110A) is used to carry out the spin transfer torque induced switching at room temperature. The offset field [as exhibited in Fig. 2(a)] is balanced by

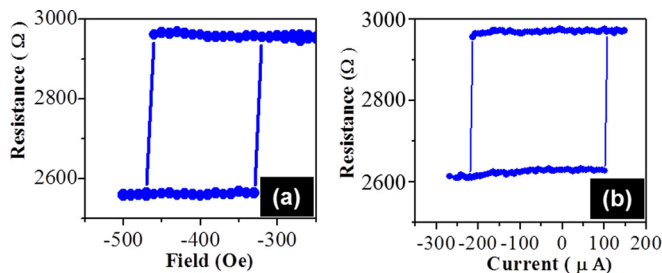


FIG. 2. (Color online) (a) Field and (b) current induced switching loop of a PMTJ device with 60 nm diameter.

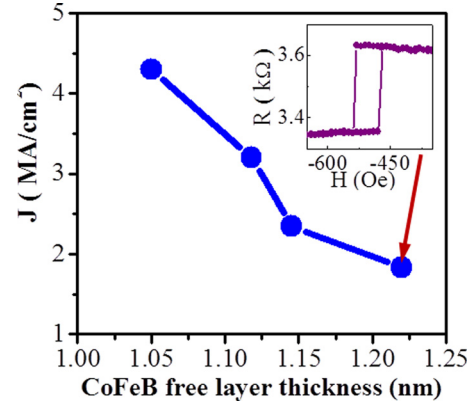


FIG. 3. (Color online) Dependence of average current density ($J = (J_{AP-P} - J_{P-AP})/2$) on the CoFeB free layer thickness for a device with 60 nm diameter. Inset is the perpendicular R - H loop of CoFeB free layer thickness of 1.22 nm.

applying an external out-of-plane field during the current switching measurement.

The switching current densities are obtained by dividing the switching current by the sample area as shown in Fig. 3. During the measurement, the positive currents correspond to electrons flowing from the pinned to the free layer, favoring the parallel state. A significant reduction in the current density for both switching directions J_{AP-P} and J_{P-AP} are observed when the free layer thickness is increased. The average switching current density $J = (J_{AP-P} - J_{P-AP})/2$ reduces by a factor of about 2.5 with moderate increase in the free layer thickness from 1.05 to 1.23 nm. The minimum switching current density of 1.87 MA/cm² is achieved for a thickness of 1.22 nm that is close to the general target of 1.0 MA/cm² for the implementation of STT based RAM.²³ The square R - H loops for CoFeB thickness of 1.22 nm shown in the inset of Fig. 3 indicates that the PMA is still dominating in CoFeB at this thickness for 60 nm circular device. The energy barrier for thermally activated switching is estimated to be 35 k_BT for this free layer thickness, where k_B and T denote the Boltzmann constant and temperature, respectively.

To understand the mechanism responsible for switching current reduction with increased CoFeB free layer thickness, we deposit a test structure with Ta (5 nm)/CoFeB (0.70 nm–1.40 nm)/MgO (0.8 nm)/Ta (5 nm) and investigate the magnetic properties of the films with different CoFeB thickness after annealing at 300 °C for 2 h. The results are shown in Fig. 4. By comparing the out-of-plane and in-plane magnetic hysteresis loops shown in Figs. 4(a) and 4(b), respectively, it can be concluded that the films exhibit strong perpendicular anisotropy with a thickness of 0.86 nm without a significant in-plane component. With an increase in the thickness to 1.06 nm, the PMA is still dominating, although some in-plane component appears. The in-plane anisotropy becomes dominating for further increasing the film thickness to 1.27 nm. The anisotropy field (H_k) estimated from the hard axis loops (in-plane loop for thickness of 0.86 and 1.06 nm and out-of-plane loop for 1.27 nm) is plotted in Fig. 4(c). The anisotropy field decreases continuously with the increase in CoFeB layer thickness and becomes negative for the CoFeB thickness of about 1.10 nm. So the transition thickness of

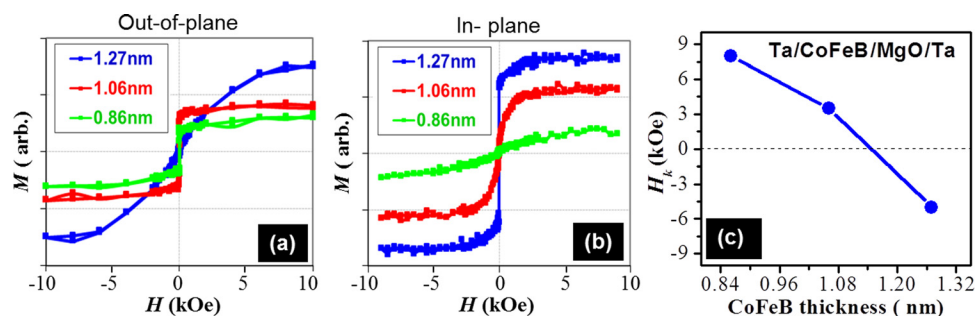


FIG. 4. (Color online) (a) Out-of-plane and (b) in-plane magnetic hysteresis loops of Ta(5 nm)/CoFeB (t nm)/MgO (0.8 nm)/Ta (5 nm) film annealed at 300 °C for 2 h. (c) Dependence of anisotropy field (H_k) as a function of CoFeB thickness.

Ta/CoFeB/MgO film in the film level is considered to be 1.10 nm, but our previous study⁶ showed that the transition thickness for the MgO/CoFeB/Ta film is about 1.5 nm. These results indicate that the strength of the PMA in CoFeB film not only depends on the adjacent layers but also depends on if the CoFeB film is situated on top or bottom of the MgO. It is also worthy to compare the film level magnetic properties with the device level ones. The R - H loop for CoFeB thickness of 1.22 nm shown in the inset of Fig. 3 exhibits square loop under perpendicular field. This explains that the CoFeB at this thickness is perpendicular in the 60 nm circular device. This discrepancy may arise from the fact that the transition thickness of CoFeB from in-plane to out-of-plane is different in device level than in the film level. The perpendicular H_c estimated from the R - H loops with CoFeB thickness of 1.22 nm (inset of Fig. 3) is significantly lower (~ 30 Oe) than with 1.0 nm (~ 75 Oe, Fig. 2). Therefore, it is evident that the PMA reduces with increasing CoFeB thickness, which eventually helps to reduce the switching current.

IV. CONCLUSION

We successfully demonstrate the development of a MgO based PMTJ structure with CoFeB free layer and CoFeB/Ru/(Co/Pd) n fixed layer. We show that the spin transfer induced switching current can be reduced by a factor of 2.5 by increasing the CoFeB free layer thickness. A switching current density of as low as 1.87 MA/cm² is achieved for a device with 60 nm diameter. The energy barrier for thermally activated switching is estimated to be 35 k_BT for this free layer thickness.

ACKNOWLEDGMENTS

The authors are grateful for the partial financial support from DARPA STT-RAM program and NSF Nano Fabrication Center at the University of Minnesota. Parts of this work were carried out in the Characterization Facility, University of Minnesota, a member of the NSF-funded Materials Research Facilities Network (www.mrfn.org) via the NSF MRSEC program under Award No. DMR-0819885.

¹J. C. Slonczewski, *J. Magn. Magn. Mater.* **159**, L1 (1996).

²L. Berger, *Phys. Rev. B* **54**, 9353 (1996).

³M. Nakayama, T. Kai, N. Shimomura, M. Amano, E. Kitagawa, T. Nagase, M. Yoshikawa, T. Kishi, S. Ikegawa, and H. Yoda, *J. Appl. Phys.* **103**, 07A710 (2008).

⁴Z. Diao, Z. Li, S. Wang, Y. Ding, A. Panchula, E. Chen, L. C. Wang, and Y. Huai, *J. Phys. Condens. Matter* **19**, 165209 (2007).

⁵S. Ikeda, J. Hayakawa, Y. M. Lee, F. Matsukura, Y. Ohno, T. Hanyu, and H. Ohno, *IEEE Trans. Electron Devices* **54**, 991 (2007).

⁶P. K. Amiri, Z. M. Zeng, J. Langer, H. Zhao, G. Rowlands, Y. J. Chen, I. N. Krivorotov, J. P. Wang, H. W. Jiang, J. A. Katine, Y. Huai, K. Galatsis, and K. L. Kang, *Appl. Phys. Lett.* **98**, 112507 (2011).

⁷Y. Huai, M. Pakala, Z. Diao, and Y. Ding, *Appl. Phys. Lett.* **87**, 222510 (2005).

⁸S. Assefa, J. Nowak, J. Z. Sun, E. O'sullivan, S. Kanakasabapathy, W. J. Gallagher, Y. Nagamine, K. Tsunekawa, D. D. Djayaprawira, and N. Watanabe, *J. Appl. Phys.* **102**, 063901 (2007).

⁹H. Zhao, A. Lyle, Y. Zhang, P. K. Amiri, G. Rowlands, Z. Zeng, J. Katine, H. Jiang, K. Galatsis, K. L. Wang, I. N. Krivorotov, and J.P. Wang, *J. Appl. Phys.* **109**, 07C720 (2011).

¹⁰X. Zhu and J. G. Zhu, *IEEE Trans. Magn.* **42**, 2739 (2006).

¹¹S. Mangin, Y. Henry, D. Ravelosona, J. A. Katine, M. J. Carey, B. D. Terris, and E. E. Fullerton, *Nature Mater.* **5**, 210 (2006).

¹²T. Seki, S. Mitani, K. Yakushiji, and K. Takahashi, *Appl. Phys. Lett.* **88**, 172504 (2006).

¹³J. H. Park, C. Park, T. Jeong, M. T. Moneck, N. T. Nufer, and J. G. Zhu, *J. Appl. Phys.* **103**, 07A917 (2008).

¹⁴C. Ducruet, B. Carvello, B. Rodmacq, S. Auffret, G. Gaudin, and B. Dieny, *J. Appl. Phys.* **103**, 07A918 (2008).

¹⁵M. T. Rahman, A. Lyle, G. Hu, W. J. Gallagher, and J. P. Wang, *J. Appl. Phys.* **109**, 07C709 (2011).

¹⁶Z. R. Tadisina, A. Natarajarathinam, and S. Gupta, *J. Vac. Sci. Technol. A* **28**, 973 (2010).

¹⁷L. E. Nistor, B. Rodmacq, S. Auffret, and B. Dieny, *Appl. Phys. Lett.* **94**, 012512 (2009).

¹⁸S. Ikeda, K. Miura, H. Yamamoto, K. Mizunuma, H. D. Gan, M. Endo, S. Kanai, J. Hayakawa, F. Matsukura, and H. Ohno, *Nature Mater.* **9**, 721 (2010).

¹⁹H. Meng, W. H. Lum, R. Sbiaa, S. Y. H. Lua, and H. K. Tan, *J. Appl. Phys.* **110**, 033904 (2011).

²⁰H. Sato, M. Yamanouchi, K. Miura, S. Ikeda, H. D. Gan, K. Mizunuma, R. Koizumi, F. Matsukura, and H. Ohno, *Appl. Phys. Lett.* **99**, 042501 (2011).

²¹J. L. Leaf and M. H. Kryder, *J. Appl. Phys.* **83**, 3720 (1998).

²²R. Sbiaa, S. Y. H. Lua, R. Law, H. Meng, R. Lye, and H. K. Tan, *J. Appl. Phys.* **109**, 07C707 (2011).

²³O. G. Heinonen and D. V. Dimitrov, *J. Appl. Phys.* **108**, 014305 (2010).

²⁴D. C. Worledge, G. Hu, D. W. Abraham, J. Z. Sun, P. L. Trouilloud, J. Nowak, S. Brown, M. C. Gaidis, E. J. O'sullivan, and R. P. Robertazzi, *Appl. Phys. Lett.* **98**, 022501 (2011).

²⁵H. Liu, D. Bedau, D. Backes, J. A. Katine, J. Langer, and A. D. Kent, *Appl. Phys. Lett.* **97**, 242510 (2010).

²⁶G. E. Rowlands, T. Rahman, J. A. Katine, J. Langer, A. Lyle, H. Zhao, J. G. Alzate, A. A. Kovalev, Y. Tserkovnyak, Z. M. Zeng, H. W. Jiang, K. Galatsis, Y. M. Huai, P. Khalili Amiri, K. L. Wang, I. N. Krivorotov, and J. P. Wang, *Appl. Phys. Lett.* **98**, 102509 (2011).

²⁷K. Kyuno, J. G. Ha, R. Yamamoto, and S. Asano, *Phys. Rev. B* **54**, 1092 (1996).

²⁸K. Mizunuma, S. Ikeda, J. H. Park, H. Yamamoto, H. Gan, K. Miura, H. Hasegawa, J. Hayakawa, F. Matsukura, and H. Ohno, *Appl. Phys. Lett.* **95**, 232516 (2009).